

# Optimizing Valve Rotational Speed Using Taguchi Techniques

**Kevin Refalo**  
FEV inc.

**Stephen Bowyer**  
FEV inc.

**Mahlon Cooper Smith IV**  
Chrysler Group LLC

**Mohammad Hijawi**  
Chrysler Group LLC

Copyright © 2010 SAE International

## ABSTRACT

As fuel economy regulations increase and customer preference shifts to smaller, higher power density engines it is more important to effectively cool certain areas of the cylinder head and valvetrain. In order to maximize valvetrain life and increase engine performance it is critical to maintain a near uniform valve seat temperature to enable proper sealing. As cylinder head bridges narrow, and the temperature increases, the water jacket may not be sufficient. An alternative method to ensuring equal temperature distribution across the valve is to promote low speed valve rotation. This will not only aid, cooling the valve seat, as well as cooling and cleaning the valves' seating surface. This paper describes the development and testing of a valve rotation study, utilizing the Taguchi approach in order to determine the most robust design.

A test stand was utilized to examine the valve rotation in which the cam was driven directly using a DC motor. The testing was performed on a type II valvetrain, using a donor cylinder head. The Taguchi based project focused on three noise factors: cylinder head machining variability, oil pressure and engine speed, as well as various control factors including valve guide clearance, valve tip surface finish, keeper geometry, valve seal tension, spring shim amount, spring design, rocker arm tab clearance, rocker arm roller radius and rocker arm pad alignment. The testing was conducted using an L18 orthogonal array and a subsequent L9 to further optimize the system.

## INTRODUCTION

This project focused on valve rotation and studied the different design features which affect valve rotation, utilizing a Taguchi approach. To date, engineers have monitored valve rotation, but were not concerned since bridge temperatures typically do not reach a point to distort the seat. However, power density increases as a result of engine boosting has increased the likelihood of the issue. This study focused on the design controls and their effect in promoting low engine speed valve rotation.

For each application, a specific amount of valve rotation is desired to maintain an even seal at the valve seat. While increasing low speed valve rotation it is important to limit the maximum valve rotation. Excessive amounts of valve rotation will result in increased wear of the mating faces, limiting engine life. For this specific study a minimum engine speed of 3500rpm was established as a target for valve rotation to begin. This was based on a customer duty cycle to ensure that over a typical driving cycle the valves would rotate at least once. A maximum value of rotation was chosen to be 15 valve rpm for all engine speeds. These valve speeds were chosen for a specific engine application, certain engines may have different requirements, but the primary objective for all designs should be to have some valve rotation in the range of typical engine operation for the 99<sup>th</sup> percentile customer.

## VALVE ROTATION THEORY

Before the SAE technical paper by Hyundai [3], little information was published describing what influences and contributes to valve rotation. Furthermore, methods to monitor valve rotation were unable to examine the rotational motion over a given lift profile to that degree of detail. The analysis in the Hyundai technical paper [3], provides an understanding of the motion, which aids in determining the design controls to influence valve rotation. Shown in Figure 1 is plot describing the valves lift motion and angular rotation as a function of crank angle.

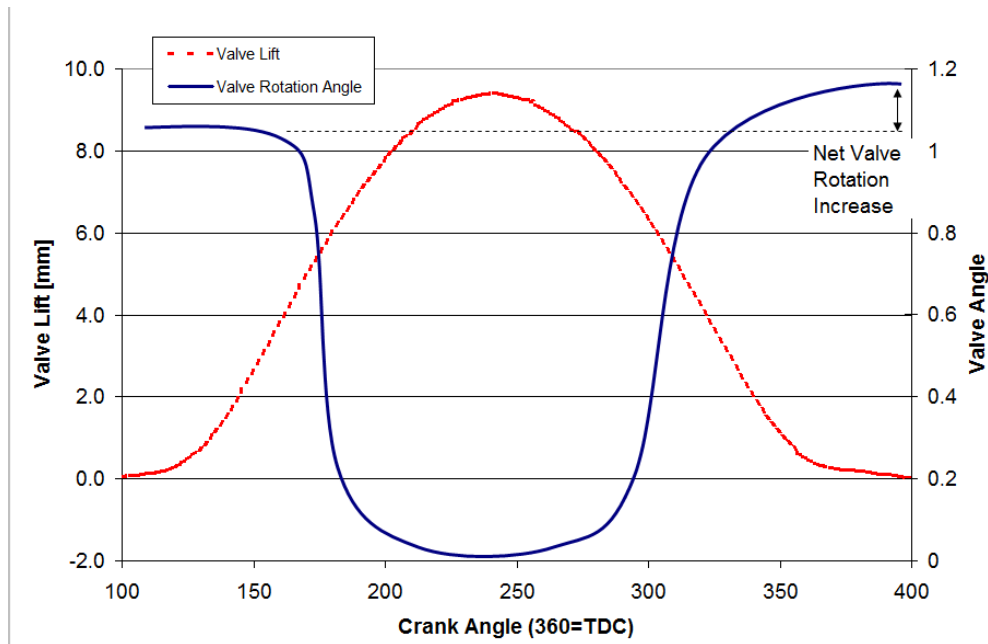
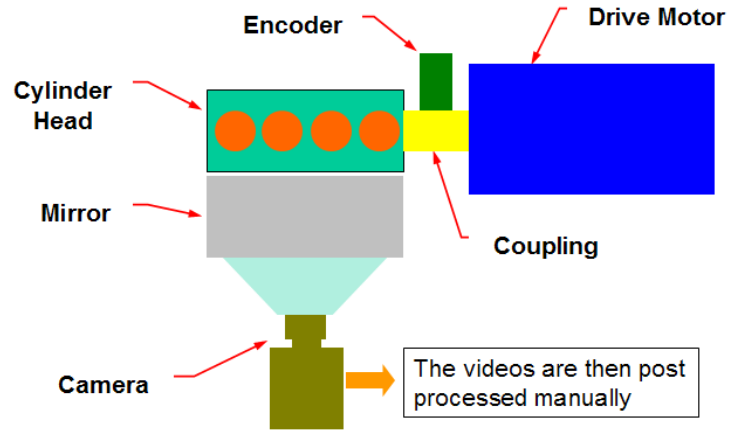


Figure 1: Typical valve motion, dashed = lift, Solid = rotation.

As the valve opens it also rotates along with the valve spring, as the valve closes it then moves back to its original position. As the speed of the motion increases, there is a greater tendency for the valve to slide at both the max lift and the closing event. This sliding motion is what provides a rotational net movement over a given lift event. What balances all of this motion is the friction between each contact interface: between the cylinder head, valve spring, valve, retainer, lock, drive mechanism, etc. Certain factors will play a greater roll in affecting the valve rotation, where others will be minimal. This study focuses on determining which interfaces provide a greater potential for increasing valve rotation.

## TESTING METHODOLOGY

To study valve rotation on the system, a bench test was constructed to drive the valvetrain while providing a method to view the valve head from the combustion chamber. A DC motor connected directly to the face of the exhaust camshaft and drove one cam at a time. This study focused on the four exhaust valves in cylinders 2 and 3. Shown in Figure 2 is a diagram of the bench test set up.



**Figure 2: Valve rotation test stand.**

The valvetrain was rotated using a DC motor that was coupled directly to the exhaust camshaft. There was no cylinder pressure or manifold pressure on the valvetrain, meaning there was no cylinder block, pistons, manifolds, etc. An oil control system was utilized to control both the temperature of the oil and the system pressure. The oil control system contained 15 gallons of oil, thus no temperature change was witnessed over the course of testing. As the valvetrain ran at a given speed, a video was recorded of the valves' rotational motion. The video was later reviewed to determine a rotational speed. By videotaping a minimum of 2 rotations and averaging the amount of time, the value increased in accuracy. Typically the valve rotation does not exceed 15 rpm, thus it does not require a high speed camera to monitor.

For a given configuration, the fixture was prepared by starting the oil control system, then ramping up the speed of the camshaft to a peak speed of 3250rpm. The speed of the cam was decreased to the first test point, 3000 engine rpm or 1500 cam rpm. At this point, video was recorded for at least 1 minute, in which either several or no valve rotation occurred. If more time was required to witness at least two valve rotations per valve, the time of recording was increased to accommodate. Every valve position (valves 2 through 6) was recorded simultaneously. The cam rpm was increased to 1750rpm, 2000rpm, 2500rpm and 3000rpm. The next setup was then configured and the process was repeated.

## TAGUCHI METHODOLOGY AND EXPERIMENTAL RESULTS

The following section will review the various parts of the Taguchi process along with chosen test factors for the orthogonal array.

## TAGUCHI IDEAL FUNCTION

Determining the ideal function is the most important step in the Taguchi process. To process the data, two approaches were taken, dynamic response and nominal the best. The nominal the best approach considered engine speed as a noise factor, thus the valve rotation speed is considered consistent across all engine speeds. A nominal value of 4 rpm is targeted through the test range, this may vary on different engine types. The second approach, dynamic response, uses the engine speed as a signal, as shown in Figure 3. The dynamic approach is more accurate in tracing a typical valve rotation trend although it has mathematical difficulties if the valves do not rotate at any speed (dividing by a zero term). The equations for both nominal the best and dynamic response are detailed in the following sections.

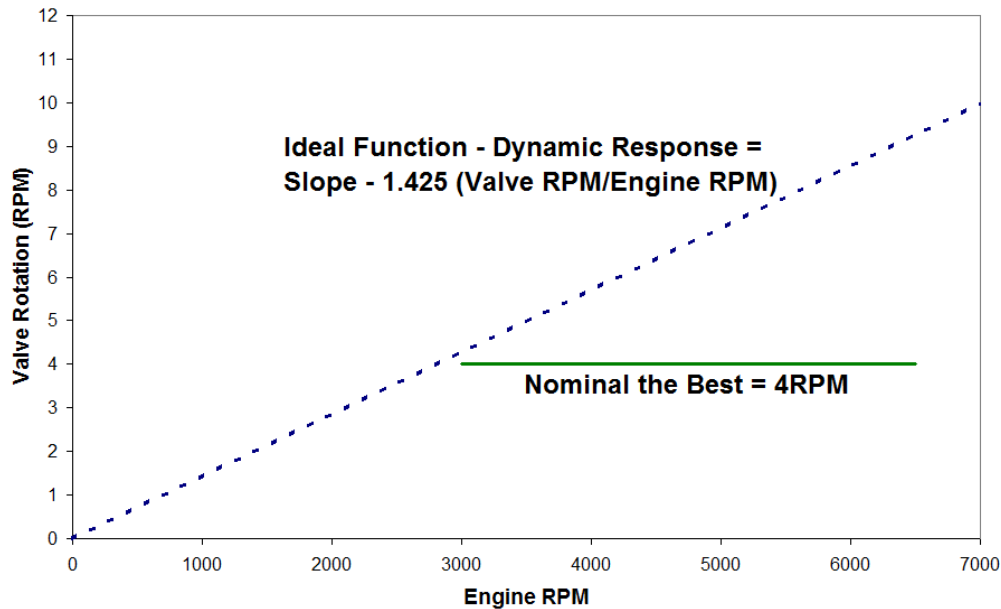


Figure 3: Ideal function.

## NOISE FACTOR SELECTION

There are several noise factors that may influence valve rotation, some of which include oil temperature, assembly variation, machining variability, valve deposits, engine vibrations and engine temperature. In order to determine which noise factors to include in the orthogonal array, a preliminary noise factor study was conducted. This study focused on three potential noise factors: oil pressure, engine speed and machining variability. The factors not under review include engine vibrations, assembly variation and engine temperature. These were deemed either unimportant or impractical to test by the team. The following paragraphs will explain why the noise factors were chosen to test and their potential impact on valve rotation.

The first noise factor, oil supply pressure, was tested as a control factor at two levels; 1.5bar and 3bar. The oil pressure was tested to determine if reducing the pressure at the valve tip by allowing the cam to compress the hydraulic lash adjuster (HLA) would aid in allowing the valve to rotate more freely.

The second noise factor chosen was engine speed (under dynamic response this is the signal input). As the engine speed increases the number of valve events per minute also increases. The levels tested in the noise factor study were; 2500rpm to 6500rpm in 500rpm increments.

The last noise factor chosen was cylinder head machining variability; this variation was captured by examining the valve rotation at different valves on the same cylinder head. The variability of one cylinder is limited, however due to testing constraints this had to be limited. To test the three noise factors, a series of tests were conducted to compare the noise factors on a factorial basis. All exhaust valves on the cylinder head were tested to examine the machining variability over all of the test runs regardless of engine speed and oil pressure.

Shown in Figure 4 is the response graph from the noise factor test. To calculate the SN ratio, a nominal the best approach was utilized. The equations for this are detailed later in this section.

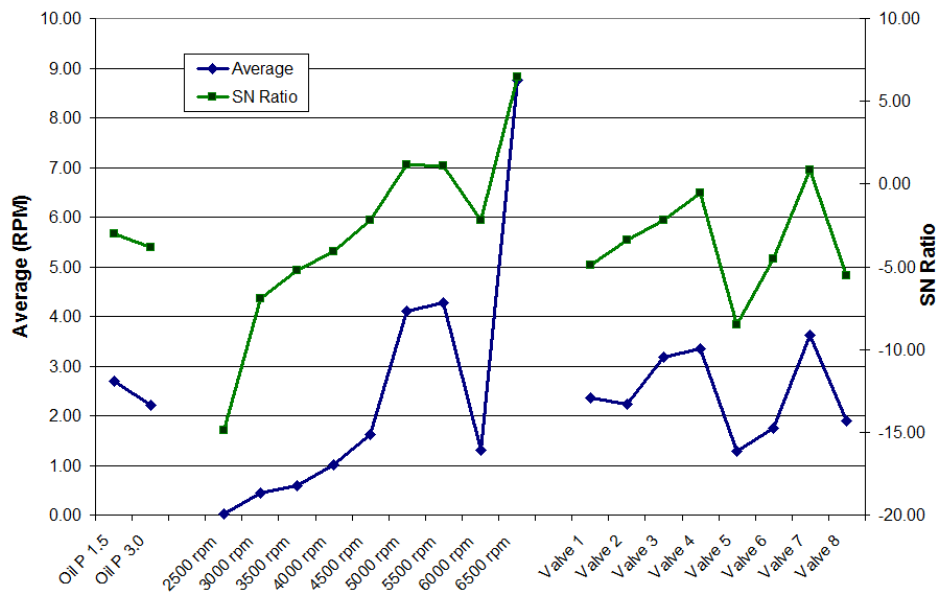


**Figure 4: Noise factor study results. – lower lines represent the average, upper lines represent the SN ratio.**

Figure 4 indicates that oil pressure had little affect on the overall valve rotation, whereas valve position and engine speed varied the rotation significantly. Both engine speed and valve position were chosen as noise factors to test over the course of the project. The average amount of valve rotation and the SN ratio follow similar trends, meaning that the standard deviation did not play a significant role in the calculation.

## CONTROL FACTOR SELECTION

The following paragraphs will discuss the control factors chosen for the orthogonal array. The reason behind choosing these control factors will also be discussed.

A single bead versus triple bead interface focused on the connection between the spring and the valve. By using a single bead retainer it forces the joint into a locked condition causing the valve to rotate, or not rotate, with the spring. By utilizing a triple bead lock the valve can rotate freely with respect to the valve spring.

The second control factor to be examined is the design of the valve spring. This was anticipated to provide significant results considering the rotational force that promotes valve rotation is created by the valve spring during compression and relaxation. To examine the valve spring, three designs were tested. The first spring, P31, has a high preload and high number of coils to provide good valvetrain system behavior. The second design has the same load factors as P31, but uses fewer coils. The third design has a lower preload than P31, but a higher spring rate.

The third control factor is the valve spring shim; this is a steel shim at the base of the valve spring to prevent wear of the aluminum cylinder head. This joint was treated as a two level control factor, with 1 or 2 spring shims. The single shim is an attempt to simulate a fixed joint between the cylinder head and the spring, where two shims will enable the spring to rotate more freely.

The fourth control factor is the valve stem seal tension. A valve stem seal pinches the valve stem in order to keep oil from the cylinder head entering the air stream of the intake or exhaust port. A valve stem seal will have an associated leak rate, which provides lubrication to the joint between the valve guide and valve. By testing the boundaries (with valve seal and without) we can determine if a higher leak rate valve seal may help valve rotation. This becomes increasingly difficult, since the valve stem seal is a contributor to overall engine emissions.

The fifth control factor to be examined is the tabs on the side of the rocker arm that help keep the rocker arm on the valve top. On previous generations of rocker arms it was observed that the tabs have an edge contact on the side of the valve. In order to eliminate the contact, a large chamfer was added to the stamping of the rocker arm body. To test the influence on valve rotation, three configurations, a rocker arm with no chamfer, chamfers on both sides, and a chamfer on one side were used. Shown in Figure 5 is a rocker arm with chamfers on both side.

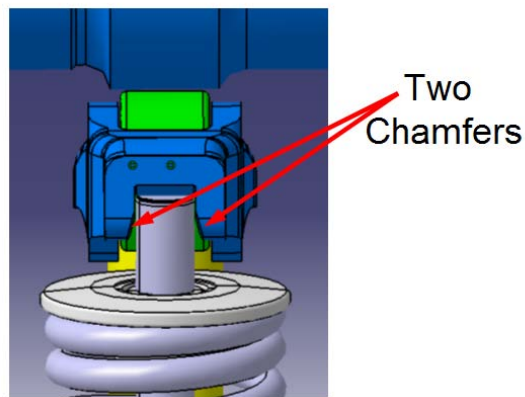


**Figure 5: Roller finger follower (RFF) to valve tip interface, also shown is the RFF to cam interface.**

The sixth control factor is the flatness of the roller on the rocker arm. Typically there is a crown on the roller to allow for self centering. To test if this plays a role in valve rotation, three different crown radii were used: flat, 350mm and 565mm.

The seventh control factor was the valve tip surface finish. Three levels were used for this control: 1.2 Ra, 0.4 Ra and 0.07 Ra.

Finally, the last control factor was the valve guide to valve stem clearance. This was a three level control factor, the min, max and nominal clearance. To summarize, Table 1 lists the different control factors and the various levels.

**Table 1: Configuration and control factors**

	Description	Level 1	Level 2	Level 3
A	Valve/Lock Interface	Single	Triple	
B	Spring Design	P31	P33	P28
C	Spring Shim	Double	Single	Single
D	Valve Seal Tension	Off	On	On
E	Rocker Arm Tabs	One Sided Chamfer	Chamfer	No Chamfer
F	Rocker Arm Roller Crown	565	Flat	350
G	Valve Tip Surface Finish	0.07	0.4	1.2
H	Valve Guide Clearance	0.0008	0.0015	0.002

## P-DIAGRAM

Now that the control factors, noises, and ideal function have been established, shown in Figure 6 is the completed P-diagram.

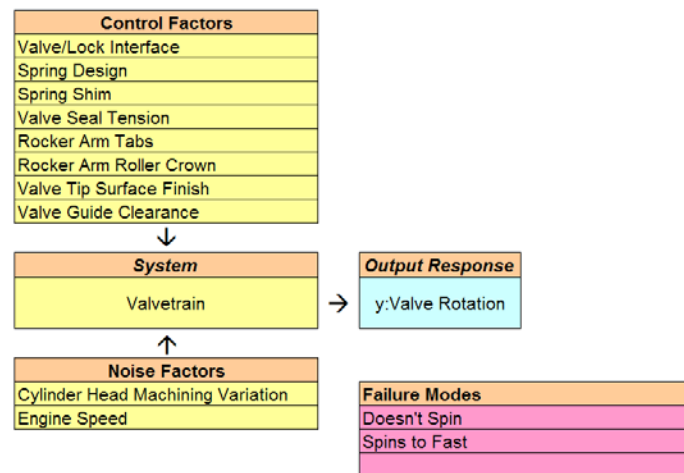


**Figure 6: L18 P-Diagram**

Since 8 control factors are identified, an L18 was selected. To conduct the tests in a timely fashion the engine speed increments focused on 3000, 3500, 4000, 5000 and 6000 rpm. Also, only cylinders 2 and 3 were tested over the orthogonal (valves 3, 4, 5 and 6). This was limited to minimize the cost of testing and the time to post-process the videos.

## EXPERIMENTAL RESULTS

Shown in Figure 7 are the test results from the orthogonal array for nominal the best. If a cell is shaded dark, then the valve was rotating. If the cell is lightly shaded, then no rotation was observed.

	3000 rpm				3500 rpm				4000 rpm				5000 rpm				6000 rpm			
	Valve 3	Valve 4	Valve 5	Valve 6	Valve 3	Valve 4	Valve 5	Valve 6	Valve 3	Valve 4	Valve 5	Valve 6	Valve 3	Valve 4	Valve 5	Valve 6	Valve 3	Valve 4	Valve 5	Valve 6
	1	0.0	0.0	0.0	0.0	0.0	0.0	0.0	0.0	0.0	0.0	0.0	0.0	0.0	0.0	0.0	0.0	0.0	0.0	0.0
2	0.0	0.0	0.0	0.0	0.0	0.0	0.0	0.0	0.0	0.0	0.0	0.0	0.0	0.0	0.0	0.0	0.0	0.0	0.0	0.0
3	0.0	0.0	0.0	0.0	0.0	0.0	0.0	0.0	0.0	0.0	0.0	0.0	0.0	0.0	0.0	0.0	0.0	0.0	0.0	0.0
4	0.0	0.0	0.0	0.0	0.0	0.0	0.0	0.0	0.0	0.0	0.0	0.0	0.0	0.0	0.0	0.0	0.0	0.0	0.0	0.0
5	0.0	0.0	0.0	0.0	0.0	0.0	0.0	0.0	0.0	0.0	0.0	0.0	0.0	0.0	0.0	0.0	0.0	0.0	0.0	0.0
6	0.0	0.0	0.0	0.0	0.0	0.0	0.0	0.0	0.0	0.0	0.0	0.0	0.0	0.0	0.0	0.0	0.0	0.0	0.0	0.0
7	0.0	0.0	0.0	0.0	0.0	0.0	0.0	0.0	0.0	0.0	0.0	0.0	0.0	0.0	0.0	0.0	0.0	0.0	0.0	0.0
8	0.0	0.0	0.0	0.0	0.0	0.0	0.0	0.0	0.0	0.0	0.0	0.0	0.0	0.0	0.0	0.0	0.0	0.0	0.0	0.0
9	0.0	0.0	0.0	0.0	0.0	0.0	0.0	0.0	0.0	0.0	0.0	0.0	0.0	0.0	0.0	0.0	0.0	0.0	0.0	0.0
10	0.0	0.0	0.0	1.3	0.0	0.0	0.0	0.0	0.0	0.0	0.0	0.0	2.8	0.0	0.0	0.0	0.0	0.1	0.1	0.0
11	0.0	2.7	0.0	1.9	0.0	2.4	0.0	5.2	4.1	3.4	0.0	5.5	0.0	11.3	0.0	0.0	0.0	0.0	0.0	0.0
12	0.0	0.0	0.0	0.0	0.0	0.0	0.0	4.5	0.0	0.0	0.0	0.0	2.5	0.0	0.0	0.0	11.3	0.0	0.0	0.0
13	0.0	0.0	0.0	0.0	0.0	0.0	0.0	3.2	0.0	0.0	0.0	1.4	0.0	2.3	7.1	0.0	12.0	0.0	0.0	0.0
14	0.0	0.0	0.0	1.3	0.0	0.0	0.0	2.5	0.0	0.0	1.4	2.0	0.0	4.6	14.1	2.5	10.0	12.0	10.0	7.1
15	0.0	0.0	0.0	0.0	0.0	1.7	1.2	0.0	0.0	0.0	4.3	4.3	10.0	10.0	7.1	0.0	10.0	15.0	10.0	12.0
16	0.0	0.0	0.0	0.0	0.0	0.0	0.0	0.0	0.0	0.0	0.0	0.0	5.5	0.0	0.0	0.0	5.2	2.4	0.0	0.0
17	0.0	0.0	0.0	0.0	0.0	0.0	0.0	0.0	0.0	1.0	0.0	0.0	0.0	7.5	0.0	0.0	3.7	0.0	0.0	0.0
18	0.0	0.0	0.0	0.0	0.0	0.0	0.0	0.0	0.0	0.0	0.0	0.0	0.0	0.0	0.0	0.0	0.0	0.0	0.0	0.0

Figure 7: L18 Orthogonal array test results.

As shown in Figure 7, the first nine test runs had limited rotation due to the single bead lock, whereas the last nine had significantly better rotation due to the triple bead lock. Discussed next are the mean and SN Ratio equations for the nominal the best analysis.

Equation 1: Nominal the best equations for signal to noise ratio and mean.

$$\bar{y} = \frac{\sum_{i=1}^n y_i}{n} = \frac{y_1 + y_2 + \dots + y_n}{n}$$

$$\sigma_{n-1}^2 = \frac{\sum_{i=1}^n (y_i - \bar{y})^2}{n-1} = \frac{(y_1 - \bar{y})^2 + (y_2 - \bar{y})^2 + \dots + (y_n - \bar{y})^2}{n-1}$$

$$S/N = \eta_{dB} = 10 \times \log\left(\frac{\bar{y}^2}{\sigma_{n-1}^2}\right)$$

Shown in Figure 8 are the response graphs from the L18 orthogonal array testing.

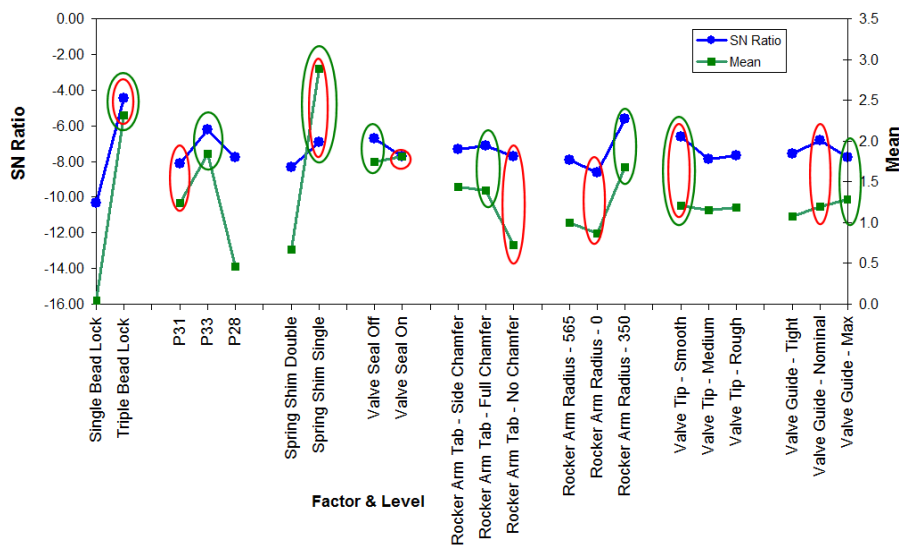


**Figure 8: L18 Orthogonal array effects plots (SN ratio above, mean below).**

As shown in Figure 8, there are no contradictions between the mean and SN plots. The initial condition is shown circled in red, while the optimum combination is circled in green. Table 2 shows each control factors SN ratio, mean and gains.

**Table 2: L18 Control factor effects table.**

S/N - 3000-6000RPM								
	A	B	C	D	E	F	G	H
1	-13.01	-8.26	-9.32	-7.72	-8.39	-9.00	-8.49	-9.45
2	-4.45	-7.34	-8.43	-9.23	-8.22	-9.72	-9.04	-7.99
3		-10.59			-9.57	-7.47	-8.66	-8.74
Δ	8.6	3.2	0.9	1.5	1.4	2.3	0.5	1.5
Mean - 3000-6000RPM								
	A	B	C	D	E	F	G	H
1	0.05	1.24	0.67	1.74	1.44	1.00	1.21	1.07
2	2.32	1.84	1.44	0.90	1.39	0.86	1.16	1.20
3		0.46			0.72	1.68	1.18	1.28
Δ	2.3	1.4	0.8	0.8	0.7	0.8	0.1	0.2

The largest gains are evident from the triple bead lock vs. the single bead lock. The second largest gains were from the spring design. The rocker arm roller radius and chamfer design also showed moderate gains. Minimal gains are noticed with the valve seal, valve guide clearance and valve tip surface finish.

From the experimental results of the L18 it is possible to predict the SN and mean gains of the optimum condition using the following equations.

**Equation 2: Prediction equation for SN ratio and mean.**

$$\hat{\eta}_{opt} = \bar{T} + (A_i - \bar{T}) + (B_i - \bar{T}) + (C_i - \bar{T}) + (D_i - \bar{T}) + (E_i - \bar{T}) + (F_i - \bar{T}) + (G_i - \bar{T}) + (H_i - \bar{T})$$

$$\bar{T} = \frac{\sum_{i=1}^n SN_i}{n} = \frac{SN_1 + SN_2 + \dots + SN_n}{n}$$

Utilizing this equation it was then possible to compare the initial condition with the optimum condition from the L18 orthogonal array. Figure 9 describes the initial combination, as well as the two optimum combinations chosen. There were two optimized combinations, to examine the benefit of the crowned roller because this would have a large cost impact on the component in this particular application. The optimized combinations were chosen to maximize the SN ratio, no combinations to maximize the average were examined since most control factors had similar effects between SN ratio and the average. The optimized combinations did have a valve stem seal, since not having a valve stem seal is unrealistic for production.

	A	B	C	D	E	F	G	H	A	B	C	D	E	F	G	H
Initial	2	1	2	2	3	2	1	1	Triple	P31	Single	On	No Chamfer	Flat	0.07	0.0008
Optimum 1	2	2	2	2	2	3	1	3	Triple	P33	Single	On	Chamfer	350	0.07	0.002
Optimum 2	2	2	2	2	2	2	1	3	Triple	P33	Single	On	Chamfer	Flat	0.07	0.002

L18 Nominal the Best Prediction and Confirmation								
	Prediction			Confirmation			Accuracy	
	S/N	Mean	% Range	S/N	Mean	% Range	S/N	Mean
Initial =	-6.0	1.5	100%					
Optimum 1	-0.7	3.8	54%	-2.7	3.5	68%	-271%	7%
Optimum 2	-3.8	3.0	77%	-2.3	3.8	65%	39%	-30%
Gain 1	5.3			3.3				
Gain 2	2.3			3.7				

**Figure 9: L18 Optimization results. Top chart is the combinations. Lower chart is the prediction, confirmation and prediction accuracy table.**

From the prediction model, shown above in Figure 9, the variability was predicted to be reduced by 46%. This is represented in the %Range column; the variability of the valve rotation speed will be reduced according to this prediction model. More importantly, the mean value for valve rotation should at least double. In order to verify the prediction model, the optimized combinations were tested. Figure 9 shows the optimized combinations and a comparison table from these findings with the predictions.

Also shown in Figure 9, two different tests were conducted to examine the best combination. From these results it was shown that the prediction model was not accurate. This was due to the dominant response from the single bead retainer. As different combinations were examined, the single bead lock eliminated any rotational benefits from the other control factors. Due to the dominant behavior of one control factor, the ability to determine the optimized combination was limited.

Another method in reviewing the data from the L18 was to examine the average amount of valve rotation over each control factor at a given speed. Plots were then created to examine the average deviation between each control factor. From this examination it was clear that the spring design, roller crown and rocker arm tab played a significant role in affecting valve rotation. There were clear increases in valve rotation from spring designs P28 to P31 and to P33. This may be attributed to the stiffness, mass, natural frequency or the number of coils in the spring. There was also a clear trend between springs P28 and P31 which can only be attributed to the natural frequency, mass and coil count since the loads of both springs are identical.

## L18 CONCLUSIONS

Although the L18 orthogonal array prediction was unable to confirm with the optimization test trials, the findings are still useful in determining the next steps. The results did show that the triple bead lock, valve spring, rocker arm roller radius and rocker arm tab chamfer play a role in aiding or causing valve rotation. The results also showed that in this system, spring shims, valve guide clearance, valve tip surface finish and the valve stem seal have little effect and should not be pursued further in determining the best possible combination for valve rotation.

## TAGUCHI EXPERIMENTAL RESULTS

The following section will review a subsequent L9 orthogonal array experiment that further examined the design parameters of valve rotation.

### CONTROL FACTORS

In order to further investigate valve rotation in the system, another orthogonal array was tested utilizing a new group of valve springs, the rocker arm roller radius, the rocker arm side tab chamfer and one new control factor. This new control factor will focus on adding a misalignment to the rocker arm and valve tip to attempt to add a torque when contacting the valve. Shown in Figure 10 is the new rocker arm pad with a machining operation to remove half of the mating surface.

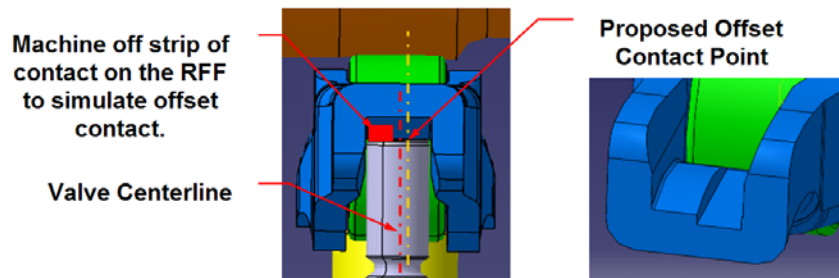


Figure 10: Rocker arm pad misalignment.

Based on the findings from the L18, triple bead locks, single spring shims were utilized in all configurations of the L9. Shown in Figure 11 is the P diagram for the L9 orthogonal array. This contains similar control factors to the L18 and the same noise factors and ideal function.

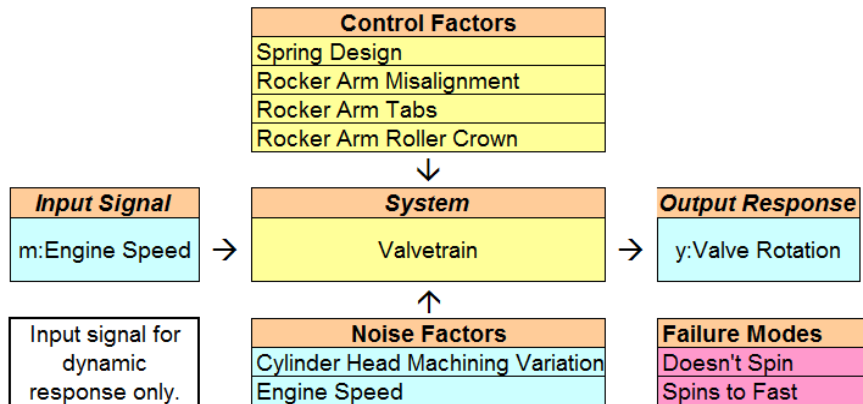


Figure 11: P-Diagram.

Shown in Figure 12 are the results from the L9 orthogonal array and the results from the nominal the best analysis.

	3000 rpm				3500 rpm				4000 rpm				5000 rpm				6000 rpm				S/N	Mean
	Valve 3	Valve 4	Valve 5	Valve 6	Valve 3	Valve 4	Valve 5	Valve 6	Valve 3	Valve 4	Valve 5	Valve 6	Valve 3	Valve 4	Valve 5	Valve 6	Valve 3	Valve 4	Valve 5	Valve 6		
1	0.0	0.0	0.0	0.0	0.8	1.0	0.4	0.0	2.3	1.7	0.6	0.0	4.6	7.2	4.0	7.2	12.0	12.0	8.0	12.0	-1.6	3.7
2	0.0	0.0	0.0	0.0	0.0	0.0	0.0	0.0	0.0	0.0	0.0	0.0	5.5	5.2	1.4	5.7	10.0	12.9	8.0	10.0	-3.3	2.9
3	0.0	0.0	0.0	0.0	1.5	1.2	1.0	1.0	3.8	2.9	2.0	2.0	0.0	3.8	5.2	2.4	8.0	13.8	8.0	9.5	-1.3	3.3
4	0.0	0.7	0.0	0.0	1.8	1.0	0.0	0.0	1.6	2.1	0.0	3.4	8.0	12.0	6.0	6.3	5.7	4.4	10.0	6.2	-0.5	3.5
5	0.0	0.0	0.0	0.0	0.0	0.0	0.0	0.0	0.0	0.0	0.0	0.0	8.0	10.6	5.5	9.5	6.0	10.0	6.7	8.6	-2.3	3.2
6	0.0	0.4	0.0	0.0	0.0	1.3	0.0	0.0	0.0	0.0	0.0	0.0	0.0	5.5	11.3	0.0	0.0	2.8	5.6	0.6	-6.5	1.4
7	0.4	0.5	0.0	0.7	1.7	4.0	0.9	0.9	1.9	2.8	0.3	2.3	3.9	6.3	6.7	8.0	8.0	13.3	15.0	8.0	-0.2	4.3
8	0.0	0.0	0.0	0.0	0.0	0.0	0.0	0.0	0.0	0.0	0.0	0.0	5.7	6.7	2.1	9.2	4.3	12.0	12.0	13.8	-3.4	3.3
9	0.0	0.0	0.0	1.0	0.0	2.1	4.1	1.9	0.0	2.7	0.0	2.9	0.0	4.3	2.7	2.4	7.5	9.2	15.0	9.2	-1.9	3.3
<b>Average</b>																					<b>-2.3</b>	<b>3.2</b>

	A	B	C	D	S/N	Mean
	1	1	1	1		
2	1	2	2	2	-3.3	2.9
3	1	2	1	3	-1.3	3.3
4	2	1	2	3	-0.5	3.5
5	2	2	1	1	-2.3	3.2
6	2	2	1	2	-6.5	1.4
7	3	1	1	2	-0.2	4.3
8	3	2	1	3	-3.4	3.3
9	3	2	2	1	-1.9	3.3
<b>Average</b>					<b>-2.3</b>	<b>3.2</b>

Figure 12: Orthogonal array test results.

Shown in Figure 13 are the response graphs for the L9 nominal the best testing.

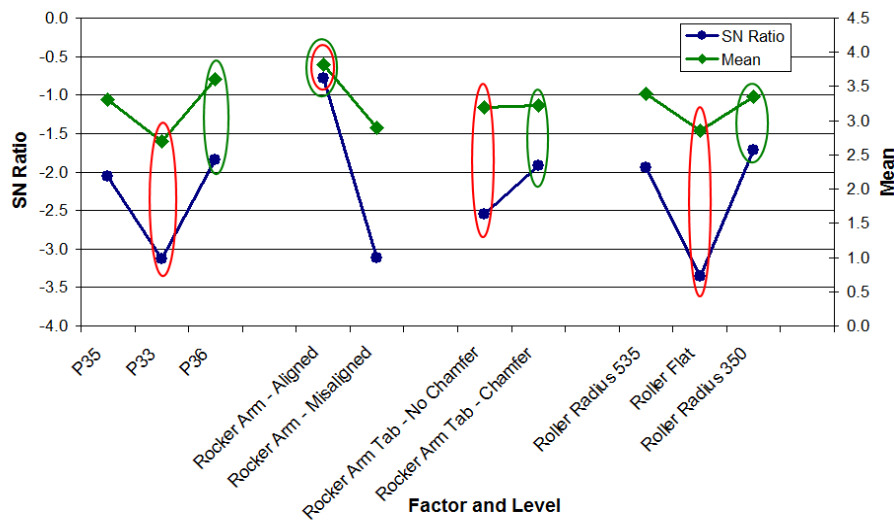


Figure 13: Effect plots, (Top = SN Ratio, Lower = Mean).

In Figure 13, the initial combination is circled in red, and the optimum combination is circled in green. From this analysis there is clear evidence that both new spring designs, P35 and P36, showed improvements. Also shown in the response graphs is that the misalignment was detrimental to valve rotation.

Since both the roller radius and the rocker arm chamfer have interactions with the misalignment cut, several optimization combinations were chosen to further examine the system. Shown in Table 3 are the optimized combinations chosen, along with a few iterations, in order to examine the effects of single factors.

**Table 3: Optimization configurations.**

L9 Optimization								
	A	B	C	D	Spring Design	Offset Rocker Contact	Rocker Arm Tabs	Rocker Arm Roller Crown
1	1	1	2	3	P35	Aligned	Chamfer	350
2	3	1	2	3	P36	Aligned	Chamfer	350
3	3	1	2	1	P36	Aligned	Chamfer	565
4	3	1	1	3	P36	Aligned	No Chamfer	350
5	3	1	2	2	P36	Aligned	Chamfer	Flat

The combinations were chosen to examine individual control factors and to ensure that no unnecessary changes were made to the system from the initial configuration. The results from the L9 optimization are shown in Figure 14.

	3000 rpm				3500 rpm				4000 rpm				5000 rpm				6000 rpm				S/N	Mean
	Valve 3	Valve 4	Valve 5	Valve 6	Valve 3	Valve 4	Valve 5	Valve 6	Valve 3	Valve 4	Valve 5	Valve 6	Valve 3	Valve 4	Valve 5	Valve 6	Valve 3	Valve 4	Valve 5	Valve 6		
Optimum 1	0.0	0.0	0.0	0.0	1.4	0.8	0.4	0.4	1.6	2.3	1.3	2.5	4.6	4.6	5.2	5.5	13.3	13.3	12.0	15.0	-1.60	4.21
Optimum 2	0.0	0.0	0.0	0.0	1.9	0.7	0.0	1.9	0.7	1.5	0.0	2.9	4.0	7.2	6.2	5.7	5.5	7.1	9.2	5.7	-0.06	3.01
Optimum 3	0.0	0.0	0.0	0.0	1.3	0.6	0.0	1.8	1.1	0.9	0.0	2.6	8.0	6.2	3.6	6.4	9.0	3.6	12.9	6.3	-1.27	3.22
Optimum 4	0.0	0.0	0.0	0.0	1.8	1.9	0.0	2.4	1.5	2.6	0.0	2.6	6.0	6.2	6.0	6.4	6.9	4.6	9.5	6.9	0.65	3.26
Optimum 5	0.0	0.0	0.0	0.0	1.3	1.1	3.3	2.1	1.0	1.3	1.8	2.5	6.0	4.6	8.2	11.3	7.5	5.5	15.0	5.5	-0.45	3.89

	A	B	C	D	S/N	Mean
Optimum 1	1	1	2	3	-1.60	4.21
Optimum 2	3	1	2	3	-0.06	3.01
Optimum 3	3	1	2	1	-1.27	3.22
Optimum 4	3	1	1	3	0.65	3.26
Optimum 5	3	1	2	2	-0.45	3.89

**Figure 14: L9 Optimization results (Shown above is the test results, shown below is the SN and mean for the results above).**

These results were promising; in some cases there was consistent valve rotation at 3500rpm. Table 4 compares the predicted values from the L9 testing to the confirmed runs in the L9 Optimization.

**Table 4: L9 Optimization comparison between predicted and confirmed results.**

3000-6000RPM								
	Prediction			Confirmation			Accuracy	
	S/N	Mean	% Range	S/N	Mean	% Range	S/N	Mean
Initial =	-2.16	4.39	100%	-2.16	4.39	100%		
Optimum 1	0.55	4.08	73%	-1.60	4.21	94%	389%	-3%
Optimum 2	0.77	4.39	71%	-0.06	3.01	78%	107%	31%
Optimum 3	0.53	4.43	73%	-1.27	3.22	90%	338%	27%
Optimum 4	0.13	4.36	77%	0.65	3.26	72%	-421%	25%
Optimum 5	-0.87	3.89	86%	-0.45	3.89	82%	48%	0%
Gain 1	2.71			0.55				
Gain 2	2.92			2.10				
Gain 3	2.69			0.89				
Gain 4	2.28			2.81				
Gain 5	1.29			1.70				

The L9 confirmation runs did not compare well with the results from the nominal the best analysis. Typically, a 30% margin of error is tolerated between the predicted value and the actual test measurement. In some cases the prediction was four times greater than the confirmed values. At this point, since all tests in the L9 configuration had some rotation, it was possible to utilize the dynamic response methodology.

### DYNAMIC RESPONSE METHODOLOGY UTILIZED ON L9 RESULTS

To further examine the results of the L9, another Taguchi analysis method was utilized; dynamic response. In this analysis, the input signal was the engine rpm. The following equations calculate the SN Ratio and Beta for dynamic response. In the equations below, M is the signal input, which in this case is the engine rpm in thousands (for example M1=3 thousand engine rpm).

**Equation 3: SN ratio and Beta calculations for the dynamic response analysis.**

$$r = \sum_{i=1}^n M_i^2 = M_1^2 + M_2^2 + \dots + M_n^2$$

$$S_T = \sum_{i=1}^n y_i^2 = y_1^2 + y_2^2 + \dots + y_n^2$$

$$S_T = S_\beta + S_e$$

$$S_\beta = \frac{\left( \sum_{i=1}^n M_i y_i \right)^2}{r} = \frac{(M_1 y_1 + M_2 y_2 + \dots + M_n y_n)^2}{(M_1^2 + M_2^2 + \dots + M_n^2)}$$

$$S_e = S_T - S_\beta$$

$$V_e = \frac{S_e}{n-1}$$

$$SN = 10 \times \text{Log} \left( \left( \frac{1}{r} \right) \left( \frac{S_\beta - V_e}{V_e} \right) \right)$$

$$\beta = \frac{\left( \sum_{i=1}^n M_i y_i \right)}{r} = \frac{(M_1 y_1 + M_2 y_2 + \dots + M_n y_n)}{(M_1^2 + M_2^2 + \dots + M_n^2)}$$

Shown in Figure 3 is the dynamic response ideal function, this trend line is more representative of typical valve rotation versus engine speed. Since this analysis follows the true trend more accurately, it should provide improved prediction capabilities. This method was not utilized earlier in the process due to its inability to handle several data points in a data set with a “zero” value, which was common when testing with the single bead lock in the L18. The data from the L9 and the corresponding optimization runs were then examined using this method. Shown in Table 5 are the results of the dynamic response analysis.

**Table 5: L9 Dynamic response calculation results.**

	$S_T$	$r$	$S_B$	$V_e$	$\beta$	S/N
1.	647.30	393	417.76	12.08	1.03	-10.68
2.	520.88	393	283.94	12.47	0.85	-12.57
3.	492.49	393	314.20	9.38	0.89	-10.83
4.	498.58	393	330.66	8.84	0.92	-10.33
5.	549.53	393	320.69	12.04	0.90	-11.86
6.	198.03	393	52.27	7.67	0.36	-18.30
7.	732.21	393	516.41	11.36	1.15	-9.46
8.	664.67	393	350.60	16.53	0.94	-12.89
9.	524.81	393	305.72	11.53	0.88	-11.88
	Average =				0.88	-12.09

Next, using these values a prediction model can be created for the confirmation runs. Shown below in Table 6 are both the prediction and confirmation outputs for both SN ratio and beta.

**Table 6: L9 Dynamic response prediction and confirmation comparison.**

3000-6000RPM						
	Prediction		Confirmation		Accuracy	
	S/N	Beta	S/N	Beta	S/N	Mean
Initial =	-12.42	0.79	-12.42	0.79		
Optimum 1	-8.19	1.11	-10.66	1.18	-30%	-6%
Optimum 2	-8.24	1.18	-9.20	0.81	-12%	32%
Optimum 3	-8.37	1.20	-10.83	0.87	-29%	27%
Optimum 4	-8.99	1.18	-8.37	0.86	7%	27%
Optimum 5	-10.34	1.05	-10.23	1.03	1%	2%
Gain 1	4.23		1.76			
Gain 2	4.18		3.22			
Gain 3	4.06		1.59			
Gain 4	3.44		4.05			
Gain 5	2.09		2.19			

This analysis showed that by utilizing dynamic response the prediction model has a significant increase in accuracy. Every prediction was within 30% of the confirmed value for SN ratio, thus deeming the confirmation and predictions successful in determining the optimized combination.

## L9 OPTIMIZATION

The L9 confirmed that the valve spring plays a significant role in increasing low speed valve rotation. This can further be attributed to the decrease in the number of coils.

The misalignment in the contact pad was detrimental to valve rotation. This was due to the method in which the alignment was implemented. Since the pad was machined away, it allowed the rocker arm to tip slightly, causing the valve to contact the side of the rocker arm. The degree in which the rocker arm was able to tip was greatly affected by the crown on the roller and the chamfers on the side of the rocker arms. This interaction did affect the ability to properly predict the SN and mean gains, but these affects were limited. To determine the effect of the rocker arm changes on an individual basis, there was a one to one comparison made during the optimization runs. Shown in Table 7 are the confirmed gains for each control factor from the optimization runs.

**Table 7: Gains for each control factor examined in the L9 Optimization.**

Control Factor	Confirmed Gains	
	S/N	Beta
<b>Valve Spring Design</b>		
P35	-0.330	0.260
P33		
P36	1.130	-0.112
<b>Rocker Arm Chamfer</b>		
Chamfer	-0.830	-0.056
No Chamfer		
<b>Rocker Arm Roller Radius</b>		
565mm Radius	-0.600	-0.155
Flat Roller		
350mm Radius	1.030	-0.223

From Table 7 it is possible to examine the gains of each control factor. For example, P35 had a decrease in SN ratio compared to P33, although there was an increase in beta. This means that the variation increased with P35, but at lower engine speeds P35 caused greater valve rotation than P33. From Table 7, the optimum combination for the SN ratio can be chosen; P36 valve spring, no chamfer on the rocker arm, with a 350mm radius rocker arm roller. This combination, however, has a lower amount of valve rotation at low speed versus the same combination with a flat rocker arm roller. Figure 15 is a plot comparing the two combinations, along with data points for each valve position.

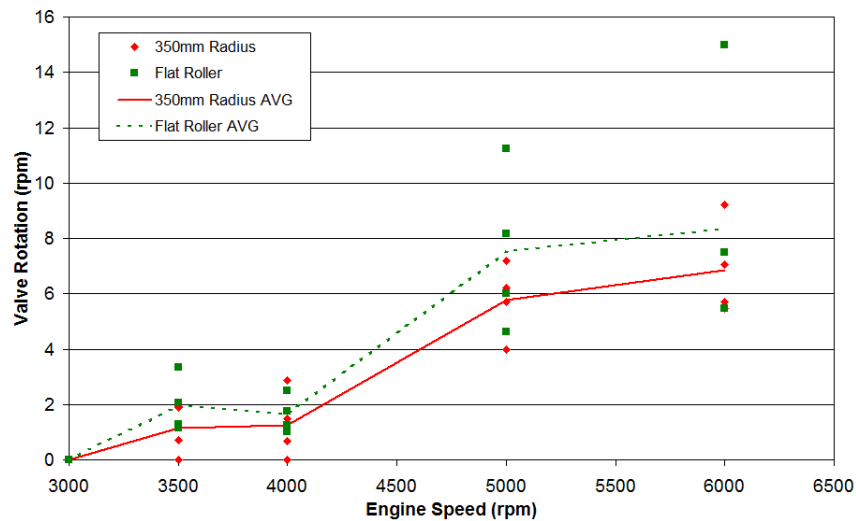


Figure 15: Average plot comparing the roller radius benefits vs. a flat roller.

## SPRING DESIGN FOR VALVE ROTATION

The testing has established that, in a given system, one of the largest single factors to promote low speed valve rotation is the valve spring design. Valve springs can be designed using various techniques with primary focus on several different factors. For high speed engines, to avoid resonance issues it is increasingly important to design a spring with a high natural frequency. In order to do this, a dual rate design is typically targeted. A dual rate spring is a spring that has a varying spring rate such that when moving from the free length to the installed height there is a large increase in natural frequency. This is created by limiting the number of active coils in the spring over the motion range of the spring, while having some coils that are inactive over the motion range. This is the same reason many high speed engines utilize a beehive spring design. A beehive spring will typically have several dead coils at the base of the spring and only one or two dead coils at the top, thereby minimizing the mass at the oscillating end of the spring. Another method in varying the natural frequency of a valve spring is to reduce mass by lowering the installed height. By reducing the mass in the active coils, the natural frequency of the spring will increase. This is limited, however, because as the installed height is decreased, there is less space for coils, thus causing the stresses in the wire to increase.

Over the course of this testing, a symmetrical spring was always utilized for the design. This enables the springs to be installed in any orientation, which is preferred from a material handling perspective. Beehive springs were tested earlier in the program and performed poorly in respect to valve rotation. The design criteria presented focuses on a symmetrical style spring, although some characteristics can be utilized in a beehive design. Shown below in Table 8 is the valve spring design table for the tested valve springs.

**Table 8: Valve spring design characteristics.**

Mubea Proposal	P28	P31	P33	P35	P36
Wire Profile	3.25 MA25	round	round	round	round
Wire Diameter a [mm]	3.60	3.30	3.40	3.30	3.40
Wire Diameter b [mm]	2.87	3.30	3.40	3.30	3.40
Inside Diameter [mm]	17.80	17.80	17.80	17.80	17.80
Outside Diameter [mm]	25.00	24.40	24.60	24.40	24.60
Number of Coils	10.40	9.10	8.80	6.85	7.75
Progr. [%]	23.2	13.0	14.6	3.7	6.8
Spring Rate at L1 [N/mm]	20.73	17.23	19.88	25.00	23.44
Spring Rate at L2 [N/mm]	23.42	29.58	33.73	28.61	30.18
Valve Closed Height [mm]	40.00	40.00	40.00	32.70	36.40
Valve Open Height [mm]	30.60	30.60	30.60	23.30	27.00
Force at L1 [N]	308	308	276	276	276
<b>Force at L2 [N]</b>	<b>528</b>	<b>528</b>	<b>528</b>	<b>528</b>	<b>528</b>
Static Stress at L1 [N/mm <sup>2</sup> ]	583	562	465	504	465
Static Stress at L2 [N/mm <sup>2</sup> ]	999	964	890	964	890
Max Solid Height [mm]	29.1	29.1	29.1	21.8	25.5
Calculated Free Length [mm]	63.3	57.9	53.9	43.7	48.2
Natural Frequency at L1 [Hz]	468	373	396	542	468
Weight [g] net	43.2	38.1	39.2	28.1	34.2

Shown in Figure 16 is an average plot comparing how each valve spring performed over comparable tests.

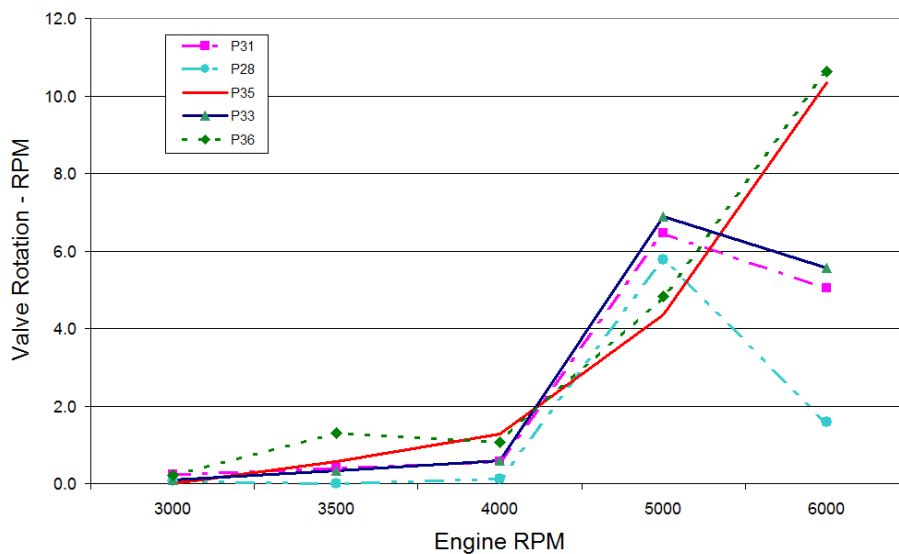


**Figure 16: Valve spring comparison, each tested with the same configuration.**

As the spring design progressed, the ability for low speed valve rotation improved. There was a significant benefit with spring design P36 at 3500 rpm, and a moderate improvement at 4000 rpm. Spring design P36 at 3500rpm has a 100% consistency for valve rotation, meaning that all valve positions tested showed valve rotation, where other springs may have 25 or 50% at most. As each spring design progressed, the number of coils in the spring decreased. This can be directly attributed to the amount of twist a spring must endure for a given lift. As a spring is compressed it has a tendency to uncoil slightly in the active coil region, causing a slight bulging in the center of the spring. This phenomena is shown in Figure 17, along with the change in max diameter for the various spring designs.

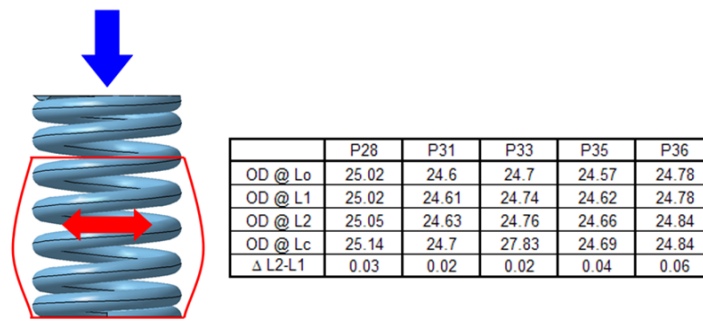


**Figure 17: Spring bulging phenomena shown left. The table to the right compares each test spring.**

As uncoiling of the spring increases, the amount of torsional energy in the spring increases and, therefore, the tendency of the valve to rotate at low speed increases. In addition, reductions in the number of coils proportionally impacts the spring mass. It was observed during the study that spring mass inversely affects valve rotation. For example, spring design P28 has a greater uncoiling tendency than P33, but rotated less. This is because the spring is 5 grams heavier, causing the frictional loads at the retainer and spring shim to increase. By lowering the valve spring mass the friction at the upper and lower interfaces can be balanced with the spring bulging phenomena to increase valve rotation at low engine speeds.

From this testing, the conclusion can be made that by reducing the mass in the system and by increasing the rotational energy in the spring, low engine speed valve rotation will increase. By decreasing the mass, the friction at the retainer will decrease, causing the valve to slip more towards the end of the valve event. In order to increase the rotational energy in the spring, the number of coils should be minimized, causing a larger twist angle per lift event.

## CONCLUSIONS

To promote low engine speed valve rotation, the following factors tested were found to positively impact valve rotation:

1. Multi bead valve lock
2. Valve spring un-coiling
3. Decreasing the number of coils in the spring
4. Decreasing the mass of the spring

The largest contributor to increasing valve rotation is the multi bead valve lock. This result is typical to most engine systems, although certain engines with a high degree of valve spring rotation may have a different result and should be verified on each application. By reducing the number of coils and mass in the valve spring, the speed at which valve rotation occurs will be lowered.

Several test factors show influence on valve rotation, although further development will be required to fully understand their effect. These include:

1. Rocker arm roller crown
2. Rocker arm pad misalignment
3. Rocker arm tab clearance

Several test factors showed no influence on valve rotation. These include:

1. Valve guide clearance
2. Valve tip surface finish
3. Valve spring shim design
4. Oil Pressure

To further examine the design controls of valve rotation there are several areas that require further examination. These include:

1. Various Valvetrain types
2. A correlation between valve spring mass, coil reduction and spring bulging
3. The effect of valve spring rotation
4. Rocker arm pad misalignment

Although the results in this study were not promising, it was observed that rocker arm pad misalignment may have a potential to assist valve rotation. However, due to cost constraints, this feature was simulated by machining the rocker arm pad. This large offset caused a tipping effect which resulted in contact between the valve and rocker arm at various points. To limit this effect, a more subtle feature should be coined, similar to the production stamping method.

Overall this testing provided a good look into the design features that effect valve rotation. By utilizing the Taguchi method, it was possible to test multiple control factors and quickly determine what affects occurred. The Taguchi approach did have limitations when examining the interactions between control factors, and certain care must be taken to ensure that there are no unknown large interactions. By using a traditional orthogonal array in a DOE, it would be possible to study the interactions more closely.

In conclusion, high-power density engines that are in demand today can greatly benefit from improved spring design in order to achieve valve rotation. To get this rotation, and gain its beneficial cooling effects, several important aspects of the spring's design should be taken into consideration. These include minimizing the mass of the spring, limiting the coil count in the spring and promoting the uncoiling effect of the spring. By taking this information into consideration while designing valve springs, valve rotation can be improved, which will maximize valvetrain life and increase the performance of today's engines.

## REFERENCES

1. Rothbart, Harold A., "CAMS Design, Dynamics and Accuracy", John Wiley Sons, 1956.
2. Wang, Yushu, "Introduction to Engine Valvetrains", SAE International, 2007.
3. Dojoong Kim, Jongwon Lee, Junghee Lee, "Effect of Valve Train Design Parameters on Valve Rotation Performance of a Diesel Engine", SAE Technical Paper F2004V281, 2004
4. Herbert C. Sumner, "Valve Rotation", SAE Technical Paper 500158, 1951.
5. A.L. Pomeroy, "Valve Rotation – Its Impact on Engine Design and Operation", SAE Technical Paper 510052, 1950.
6. Genichi Taguchi, Subir Chowdhury, Yui Wu, "Taguchi's Quality Engineering Handbook". John Wiley & Sons, 2004.

7. Dale Besterfield, Carol Besterfield-Michna, Glen Besterfield, Mary Besterfield-Sacre, "Total Quality Management". Prentice Hall, 2003

## **ACKNOWLEDGMENTS**

This testing was performed courtesy of Mubea inc. at their development facility in Auburn Hills, Michigan. The valve springs were also designed and produced by Mubea Inc.